

IV-1

**THERMODYNAMIC PROPERTIES OF MIXED ALLOYS OF GOLD-  
75/PALLADIUM-25 AND IRON**

By

J. Brian Balta

John R. Beckett

Paul D. Asimow

**ABSTRACT**

Alloys of gold and palladium are commonly used during petrology experiments as a method of minimizing the loss or gain of hydrogen from samples being held at high temperature and high pressure. The presence of palladium causes the alloy to react with any iron present in the sample and will cause loss of iron during the experiment if appropriate steps are not taken to minimize this problem. We have produced a thermodynamic calibration for the mixing of  $\text{Au}_{75}\text{Pd}_{25}$  with iron across the range of oxygen fugacities and iron activities of interest for petrological and metallurgical applications. This calibration can be used for preparation of capsules to maintain samples with little to no iron loss, and also provides a method for buffering the oxygen fugacity of samples when other oxygen buffers are not present. We have also observed internal oxidation of iron through this alloy during experiments, suggesting that oxygen can in fact be transferred across capsule boundaries during high-temperature experiments.

## 1. INTRODUCTION

The application of experimental petrology, a science rooted in classical thermodynamics, to understanding rock-forming processes in the present and past on Earth and other worlds requires production of equilibrated samples covering a considerable range of temperatures, pressures, and compositions. Studying high-temperature and high-pressure metamorphism and melting of rocks involves special challenges because it can be difficult to keep a sample effectively isolated from its surroundings for durations sufficient to approach equilibrium. Encasing the experimental charge in a capsule of a precious metal with a high melting point is the preferred method of performing these experiments. Capsules of Pt, Au, and Ag are among the most common materials used in capsule construction (e.g., Chou, 1986; Kawamoto and Hirose, 1994). However, at the temperatures of geologic interest, interaction between the capsules and the sample and diffusion of elements through the capsules appears to be commonplace. Thus, a wide variety of techniques have been developed to attempt to better isolate experimental charges from their surroundings under extreme conditions.

For simple melting experiments, platinum appears to be a good candidate as a capsule material due to its high melting point and lack of oxidation (which is generally thought to be prerequisite for solution into silicate and oxide liquids or minerals) at high temperature. However, Pt capsules have a number of disadvantages, including a high diffusivity of volatile elements and a tendency to alloy with iron (Kawamoto and Hirose, 1994). For volatile-bearing experiments, gold capsules are often used, as gold appears to show the slowest diffusion of hydrogen at high temperature among the commonly used metals (Chou, 1986; Truckenbrodt and Johannes, 1999). The main disadvantage of Au is

that its melting point is low compared with the temperatures that are required for typical silicate melting on Earth (Okamoto and Massalski, 1985). Thus, an alloy of Au doped with palladium is commonly used in an effort to obtain the benefits of slow diffusion of hydrogen at temperatures where pure Au is not suitable.

Pd-doped metal capsules have a notable disadvantage: like capsules made of Pt, Pd-doped capsules will react with Fe-bearing samples and can absorb a significant amount of Fe from the experiment, causing a number of problems by significantly changing the equilibrium chemistry (Hall et al. 2004).

A number of techniques have been applied to avoid Fe loss to Pt- or Pd-bearing capsules. These include graphite capsule linings (e.g., Medard et al., 2008), oxidizing conditions (Hall et al., 2004), and doping of capsules with Fe before use in experiments (e.g., Aubaud et al. 2008). Fe-doping is, in principle, the most flexible of these methods, since graphite linings or highly oxidizing conditions are limited to particular oxygen fugacity conditions. Experimentation with typical Fe-bearing geologic samples at the conditions of interest in the mantle requires work under a variety of oxygen fugacity conditions, with variable amounts of Fe and not necessarily at graphite saturation.

Fe-doping a capsule such that it will not exchange significant quantities of Fe with a particular experimental charge requires pre-saturating the capsule with the right amount of Fe in advance. That implies both knowing the correct Fe concentration and knowing what pre-saturation conditions and protocol will yield that concentration. Previously, for AuPd alloys, only ad-hoc methods were available, such as presaturation of capsules at ambient pressure and elevated temperature in a controlled oxygen fugacity gas mixture using liquids similar to the ones expected in the high-pressure experiments

(e.g., Aubaud et al. 2008; Botcharnikov et al. 2008). Shifting of pressure, temperature, and liquid or mineral composition from the presaturation conditions to the run conditions, however, can change the oxygen fugacity that is required to produce the  $\text{Fe}^{3+}/\text{Fe}^{2+}$  ratio in the liquid and, in turn, the Fe content of the capsule in equilibrium with that liquid.

Kessel et al. (2001) presented a detailed calibration for the dissolution of Fe into Pt capsules, which can be used as a method for preparation of capsules that will minimize Fe exchange with geologic samples under very general conditions. Because AuPd alloys are superior for volatile-bearing experiments, a similar calibration for that system is needed for work with  $\text{H}_2\text{O}$  and Fe-bearing charges. This requires a calibration defining the Fe content of AuPd capsules as a function of the activity of Fe and a method for determining the activity of Fe in the desired experimental charge as a function of liquid composition, pressure, temperature, and oxygen fugacity. Since thermodynamic calculators are available to calculate the Fe activity in silicate liquids, the essential need is for an activity-composition model for Fe-Au-Pd alloys. Here we present a calibration along a binary subsystem of this ternary, along the join from Fe to 75% Au, 25% Pd (weight units). The method and the thermodynamic basis of this work parallels closely the approach of Kessel et al. (2001) for the Fe-Pt system.

## 2. METHODS

Experiments were conducted following the techniques outlined by Chamberlin et al., (1993) and Kessel et al. (2001) in a 1 atm. Deltech DT-31 furnace using a mixture of  $\text{H}_2$  and  $\text{CO}_2$  gases to control the  $f\text{O}_2$ . Gas mixtures were set using an yttria-doped zirconia solid electrolyte oxygen sensor calibrated at fixed points against air and the iron-wüstite buffer. The oxygen sensor readings were maintained to within  $\pm 3$  mV, which

should maintain the  $f_{\text{O}_2}$  to within  $\pm 0.1 \log_{10}$  bars ( $1\sigma$ ). Temperatures were measured using a type S (Pt-Pt<sub>90</sub>Rh<sub>10</sub>) thermocouple, and are expected to be accurate and constant to  $\pm 1^\circ\text{C}$  ( $1\sigma$ ).

For each experiment, the sample was prepared by cutting a thin strip of laboratory grade Au<sub>75</sub>Pd<sub>25</sub> (confirmed accurate to within 1% by repeated electron microprobe analysis). The strip was packed in laboratory grade Fe<sub>2</sub>O<sub>3</sub> and compressed into a pellet. The pellet was placed into an alumina crucible and suspended in the hot spot of the vertical tube furnace (Chamberlin et al., 1993). The experiments were run at temperatures of 1125 °C, 1190 °C, and 1240 °C. The upper limit was set by the solidus temperature of this alloy, ~1250 °C. Most experiments were conducted at 1190 °C, which is above the liquidus of common basaltic liquids often used for pre-saturation. Other experiments were conducted at 1125 °C and 1240 °C to evaluate the effect of temperature changes on the composition. All experiments were conducted at  $f_{\text{O}_2}$  and temperature conditions such that the stable oxide phase should be either magnetite or wüstite. Experiments were run for a minimum of 48 hours for the two higher temperatures and 72 hours at the lowest temperature. While diffusion of metals in AuPd capsules is not as well calibrated as diffusion of Fe in Pt (Berger and Schwartz, 1978), in all cases these times were sufficient to fully convert the oxide pellet to either FeO or Fe<sub>3</sub>O<sub>4</sub> and to homogenize the metal strip to better than the standard error of the electron microprobe measurement. To confirm equilibrium, a reversal experiment was conducted by placing two strips in iron oxide simultaneously under reducing conditions, retaining the second strip after the experiment, and repeating the experiment by placing the extra strip back into iron oxide under oxidizing conditions with a fresh strip of metal for comparison. Experiments were

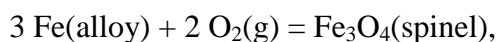
quenched by removing the crucible from the furnace and cooling it in air; cooling times were on the order of 10's of seconds. This time was rapid enough that no obvious conversion of FeO or Fe<sub>3</sub>O<sub>4</sub> to Fe<sub>2</sub>O<sub>3</sub> was observed, and no significant changes in alloy composition were expected.

Completed samples were removed from their pellets manually while wearing gloves to avoid contamination. Strips were cut into multiple pieces, with at least 1/3 of the original strip stored for reference. Other strips were mounted in epoxy and polished using alumina pads and diamond pastes. The strips were oriented at angles relative to the polishing surface, to expose a full transect across the metal strip. Samples were carbon coated and analyzed using the JEOL JXA-8200 electron microprobe at the California Institute of Technology in wavelength dispersive mode. Samples were analyzed using focused beams with an accelerating voltage of 15 kV and currents of 30-40 nA. Between 10 and 25 spots were analyzed for each sample, typically covering 2 different cuttings from the same experiment. No obvious variation was observed either on transects or on different cuttings from the same experiment, strongly suggesting that the samples reached equilibrium. Fe oxides were also analyzed by electron probe with Fe standardized on Fe metal, allowing calculation of the oxidation state of the Fe by assuming that the mass deficit is entirely due to oxygen.

### 3. RESULTS

Au<sub>75</sub>Pd<sub>25</sub> alloys reacted with the oxides at temperature and produced final equilibrated alloys of Fe mixed with AuPd. Compositions of the experimental alloys are given in Table 1 and displayed as a function of  $fO_2$  in Figure 1. Smooth trends in Fe content versus  $fO_2$  are observed at each temperature.

Calculation of an equilibrium composition between a silicate liquid and a capsule alloy requires conversion of oxygen fugacity information to an activity of Fe. The stable Fe oxide phase in each experiment was either wüstite or magnetite. The thermodynamic properties of both phases have been well calibrated previously and allow conversion to Fe metal activities. Neither phase is expected to be fully stoichiometric under these conditions. However, as pointed out by Kessel et al. (2001), magnetite approaches nominal stoichiometry as the temperature decreases. The difference between stoichiometric magnetite and the likely actual composition at these temperatures should be minimal, and thus magnetite was assumed to be stoichiometric. We expect that the activity of  $\text{Fe}_3\text{O}_4$  in the spinel phase component differs from unity by no more than 1%. The activity of Fe in magnetite can then be calculated using the reaction



whose equilibrium constant is given by:

$$K_{Mt} = \frac{a_{\text{spinel}}^{\text{Fe}_3\text{O}_4}}{\left(a_{\text{alloy}}^{\text{Fe}}\right)^3 \left(f\text{O}_2\right)^2} . \quad (1)$$

The equilibrium constant  $K_{Mt}$  was calculated from the values of the free energy of formation given by Kessel et al. (2001) using linear interpolation between the temperatures at which  $\Delta G^0$  is reported in that work. The values of this parameter are well fit by a linear function of temperature and the error in this interpolation should be minimal.

Wüstite is expected to vary significantly in its stoichiometry across these oxygen fugacities. The activity of FeO is therefore significantly different from unity under the conditions of these experiments and the activity of Fe will be a function of the

composition of this mineral. To calculate an activity of FeO, we repeated the Gibbs-Duhem integration of Darken and Gurry (1945) at the temperatures and oxygen fugacities of interest. Specific details of the integration are given in Kessel et al. (2001). After calculation of the variation in activity of FeO across the range sampled in our experiments, the activity of Fe was calculated using the reaction



whose equilibrium constant is

$$K_{Wü} = \frac{a_{wüstite}^{FeO}}{(a_{alloy}^{Fe})(fO_2)^{1/2}} \quad (2)$$

The equilibrium constant  $K_{Wü}$  was calculated via linear interpolation from the equilibrium constants given in Darken and Gurry (1945) at various temperatures. Calculated activities of Fe give a smooth trend versus measured alloy composition, as shown in Figure 2.

In addition to deviation of the oxide phases from nominal oxygen stoichiometry, solution of any other components, including Au or Pd, would lead to errors by decreasing the activity of Fe in that oxide. A simple check can be performed from our data to verify that this effect is negligible. There is no reason to expect that the solubility of Au and Pd in Fe oxides will be identical; therefore, a change in the ratio of Pd to Au in the samples would potentially reflect loss of one of these species to the oxide. Only 1 sample showed a measurable difference: run 12, which was the most reducing experiment conducted at 1240 °C (Table 1). However, this sample still plots on the trend in Fe activity versus composition defined by the remaining samples, so we suggest the effect here is likely limited. Future experiments conducted at conditions more reducing than this experiment

may find this effect to be a greater concern. Interestingly, the Pd/Au ratio in the analyzed metal increased in this experiment, suggesting preferential incorporation of Au into wüstite. Since the Au-Fe miscibility gap is larger than that in the Pd-Fe system (Okamoto et al., 1986), one might have expected the opposite behavior, with preferred solution of Pd into the Fe-oxide phase. The analysis of the Au/Pd ratio of our final alloys is also an important check for the application of our results to mixing along the pseudo-binary join between Fe and  $\text{Au}_{75}\text{Pd}_{25}$ .

We conducted a reversal experiment from reducing conditions to very oxidizing conditions to verify that the samples were able to achieve equilibrium on the timescales of the experiment. Beginning with pure  $\text{Au}_{75}\text{Pd}_{25}$ , the reducing step should create an alloy with a high concentration of Fe, which must then diffuse out during the oxidizing step. Reaching the same composition as achieved by diffusing a small concentration into initially pure  $\text{Au}_{75}\text{Pd}_{25}$  under oxidizing conditions documents a reversed equilibrium. Sample 8R reflects the final analysis of the reversed sample, which achieved an identical composition to Sample 8, run at the same time. The reversal experiment produced an unexpected result, however. It was expected that the added iron would diffuse out of the metal and move back into the large pool of Fe oxide. However, instead of leaving the metal, the extra Fe nucleated crystals of Fe oxide within the solid metal layer (Figure 3). Examination of the orientation of the polished surface and polishing to different levels within the sample verified that the Fe oxide grains were isolated within the metal. This Fe oxide was verified by electron probe totals to be magnetite, which was the stable phase under those conditions. Previously, the species capable of diffusing through capsules was questionable, as the analysis of specific diffusing species is complicated by the difficulty

in preparing experiments with known amounts of oxygen and other volatiles (Truckenbrodt and Johannes, 1999). This experiment verifies that oxygen itself is able to be transferred across capsule boundaries in high-temperature experiments, although it remains possible that the diffusing species is not atomic oxygen but could instead be an oxide species such as CO<sub>2</sub> or H<sub>2</sub>O. The diffusion of oxygen-containing species should be considered a method of changing the oxygen fugacity of samples during unbuffered experiments even when volatiles or high metal concentrations are not present.

#### 4. ACTIVITY-COMPOSITION MODEL

The Au-Pd-Fe system shows negative deviations from ideal solution of Fe (that is, the activity of Fe is less than the mole fraction of Fe) over the full compositional range examined here; the deviation from ideality decreases with increasing Fe content. The deviation from ideality is smaller than that seen in the Pt-Fe system (Kessel et al. 2001). To model this system in full would require construction of a ternary solution model, which would require more data covering other Pd/Au ratios. However, in the more limited case of this single Pd/Au ratio, we can produce a simplified (pseudobinary) model where the Au and Pd are treated as a single end member into which Fe is dissolving. We caution that application of this solution model is only applicable for Au<sub>75</sub>Pd<sub>25</sub> alloys reacting with Fe, but this is a common choice of capsule material and so this preliminary calibration should prove useful on its own.

We modeled our data by fitting it to an asymmetric regular solution model of the form:

$$RT \ln \gamma_{\text{Fe}} = [W_{\text{G1}} + 2(W_{\text{G2}} - W_{\text{G1}})X_{\text{Fe}}](X_{\text{AuPd}})^2 \quad (3)$$

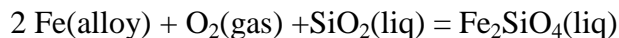
$$RT \ln \gamma_{\text{AuPd}} = [W_{\text{G1}} + 2(W_{\text{G2}} - W_{\text{G1}})X_{\text{Fe}}](X_{\text{Fe}})^2 \quad (4)$$

$$X_{\text{Fe}} = 1 - X_{\text{AuPd}}, \quad (5)$$

where  $\gamma$  is the activity coefficient for the component in the solution,  $X$  is the measured mole fraction of the component, and  $W_{G1}$  and  $W_{G2}$  are temperature-and-composition-independent Margules parameters. We attempted to fit our data to a symmetric regular solution, where  $W_{G2} = W_{G1}$ , but the quality of the fit was poor compared to that in the asymmetric case including both parameters. Fit values of these parameters are  $-45.0 \pm 1.79$  kJ/mol and  $+19.5 \pm 7.70$  kJ/mol, respectively (the errors are obtained by Monte Carlo simulation, varying all independent and dependent data parameters over Gaussian distributions). These Margules parameters have lower absolute values than those for the Pt-Fe system, again consistent with a less negative deviation from ideality and lower solubility of Fe in these AuPd alloys. The fit is compared to our measured data in figure 4, and appears to be reasonable within the margin of error across the full compositional range.

## **5. APPLICATION OF SOLUTION MODEL TO PREPARATION OF CAPSULES FOR FE-BEARING EXPERIMENTS**

Prevention of Fe-loss to the capsule in melting experiments requires conversion from an activity-composition relationship measured in a metal alloy to one calculated in the silicate liquid in question. The thermodynamics-based MELTS algorithm (Ghiorso and Sack, 1995) can be used as a method of calculating activities of oxide-components within any silicate liquid for which it is calibrated. A full explanation of this procedure is given in Kessel et al. (2001) and is summarized here. The MELTS algorithm returns values of  $\Delta G^0$  and activity for the liquid components  $\text{Fe}_2\text{SiO}_4$  and  $\text{SiO}_2$  that can be used to calculate the activity of Fe using the reaction



for which the law of mass action states, at equilibrium,

$$\Delta G = 0 = \Delta G^0 + RT \ln\left(\frac{a_{\text{Fe}_2\text{SiO}_4}^{\text{liq}}}{a_{\text{SiO}_2}^{\text{liq}} (a_{\text{Fe}}^{\text{alloy}})^2 f_{\text{O}_2}}\right) \quad (6)$$

However, the values of  $\Delta G^0$  returned by MELTS are apparent values relative to the elements at 298.15K and 1 bar. The standard state must therefore be corrected to the temperature of interest, using values for the thermodynamic properties of Si, Fe, and O from Robie et al. (1978) and the expression shown in Kessel et al. (2001).

Figure 5 shows an example calculation of the capsule alloy composition that would be in equilibrium with Kilauea 1919 basalt across a range of oxygen fugacities at 1 bar pressure and 1190 °C (all  $f_{\text{O}_2}$  values are relative to the QFM buffer). A single experimental value is presented based on actual capsule pre-saturation work using this basalt as a starting material ( $X_{\text{Fe}} = .114$  at QFM-1.6). Table 2 gives the values extracted from MELTS that are necessary for this calculation from Kilauea 1919 basalt. This calculation shows how large the shifts in alloy composition can be if capsule material is not pre-saturated at the correct level. Under oxidizing conditions, a change of 1 log unit in oxygen fugacity can correlate with a change in the alloy composition by a factor of 2. Under more reducing conditions, a change in 1 log unit in  $f_{\text{O}_2}$  can still change the equilibrium alloy composition by a factor of 1.5. Thus, pre-saturation of a capsule with an inappropriate Fe content can still lead to large shifts in oxygen fugacity and Fe content during experiments, even under oxidizing conditions or in experiments with lower Fe contents. Conversely, the presence of an appropriately pre-saturated AuPd capsule can provide a strong compositional buffer across a large range of oxygen fugacities, as a

significant and measureable change in alloy composition would be required for a sample to move to a different oxygen fugacity (Figure 5). While the buffering capacity of a capsule in any experiment depends on the ratio of the capsule mass to the sample mass, under all but the most oxidizing conditions or in very low-Fe samples, a variation of a single log unit in  $fO_2$  should produce significant changes in the composition of the equilibrium alloy and likely also significant shifts in the Fe content of the sample.

Continued refinements and improvements of the MELTS algorithm will also improve the reliability of this calculation. The pMELTS algorithm (Ghiorso et al., 2001) can be used for more accurate calculation of the thermodynamic properties of liquids at pressures up to 3 GPa. Water in particular can be expected to have a significant impact on the activities of silica and possibly iron in the liquid phase (e.g., Chapter 2) and thus must be considered in any calculation. The `adiabat_1ph` front-end for the various MELTS algorithms (Smith and Asimow, 2005) can be used to return the thermodynamic parameters in question for liquids calculated by any of the algorithms, and instructions for this process can be obtained from the authors.

## 6. ACKNOWLEDGEMENTS

The authors would like to thank June Wicks and Andrew Matzen for their help with the 1-atmosphere furnace experiments. This work was supported by the NSF Ocean Sciences Marine Geology and Geophysics program, grant numbers OCE-0241716 and OCE-0550216.

**REFERENCES**

- Aubaud, C., Hirschmann, M. M., Withers, A. C., and Hervig, R. L. (2008) Hydrogen partitioning between melt, clinopyroxene, and garnet at 3 GPa in a hydrous MORB with 6 wt.% H<sub>2</sub>O. *Contrib. Mineral. Petr.* **156**, 607-625.
- Berger, D. and K. Schwartz (1978) Zur Fremddiffusion in Platin. *Neue Huette* **23**, 210-212.
- Botcharnikov, R. E., Almeev, R. R., Koepke, J., and Holtz, F. (2008) Phase relations and liquid lines of descent in hydrous ferrobalt - implications for the Skaergaard intrusion and Columbia River flood basalts. *J. Petrol.* **49**, 1687-1727.
- Chamberlin, L., Beckett, J. R., and Stolper, E. M. (1994) Pd-oxide equilibration: a new experimental method for the direct determination of oxide activities in melts and minerals. *Contrib. Mineral. Petr.* **116**, 169-181.
- Chou, I.-M. (1986) Permeability of precious metals to hydrogen at 2 kb total pressure and elevated temperatures. *Am. J. Sci.* **286**, 638-658.
- Darken, L. S. and R. W. Gurry (1945) The system iron-oxygen. I. The wüstite field and related equilibria. *J. Amer. Chem. Soc.* **67**, 1398-1412.
- Garcia, M. O., Pietruszka, A., and Rhodes, J. M. (2003) A petrologic perspective of Kilauea volcano's summit magma reservoir. *J. Petrol.* **44**, 2313-2339.
- Ghiorso, M. S. and R. O. Sack (1995) Chemical mass-transfer in magmatic processes IV. A revised and internally consistent thermodynamic model for the interpolation and extrapolation of liquid-solid equilibria in magmatic systems at elevated temperatures and pressures. *Contrib. Mineral. Petr.* **119**, 197-212.

- Ghiorso, M. S., Hirschmann, M. M., Reiners, P. W., and Kress, V. C. (2001) The pMELTS: a revision of MELTS for improved calculation of phase relations and major element partitioning related to partial melting of the mantle to 3 GPa. *Geochem. Geophys. Geosyst.* **3**, 1030.
- Hall, L. J., Brodie, J., Wood, B. J., and Carroll, M. R. (2004) Iron and water losses from hydrous basalts contained in Au<sub>80</sub>Pd<sub>20</sub> capsules at high pressure and temperature. *Mineral. Mag.* **68**, 75-81.
- Medard, E., McCammon, C. A., Barr, J. A., and Grove, T. L. (2008) Oxygen fugacity, temperature reproducibility, and H<sub>2</sub>O contents of nominally anhydrous piston-cylinder experiments using graphite capsules. *Am. Mineral.* **93**, 1838-1844.
- Kawamoto, T. and K. Hirose (1994) Au-Pd sample containers for melting experiments on iron and water bearing systems. *Eur. J. Mineral.* **6**, 381-385.
- Kessel, R., Beckett, J. R., and Stolper, E. M. (2001) Thermodynamic properties of the Pt-Fe system. *Am. Mineral.* **86**, 1003-1014.
- Okamoto, H. and T. Massalski (1985) The Au-Pd (Gold-Palladium) system. *J. Phase Equilib.* **6**, 229-235.
- Okamoto, H., Massalski, T., Swartzendruber, L., and Beck, P. (1986) The Au-Fe system. *J. Phase Equilib.* **7**, 522-522.
- Robie, R. A. and B. S. Hemingway (1978) Thermodynamic properties of minerals and related substances at 298.15 K and 1 bar (105 Pascals) pressure and at higher temperatures. *Geological Survey Bulletin* **1452**, 456 p.
- Smith, P. M. and P. D. Asimow (2005) Adibat\_1ph: A new front end to the MELTS, pMELTS, and pHMELTS models. *Geochem. Geophys. Geosyst.* **6**, Q02004.

Truckenbrodt, J. and W. Johannes (1999) H<sub>2</sub>O loss during piston-cylinder experiments.

*Am. Mineral.* **84**, 1333-1335.

## TABLES

Table 1

Run Number	T (°C)	Log ( $fO_2$ ), bars	Fe Oxide Phase	$X_{Fe}$	$1\sigma$	$a_{Fe}$	Pd/Au	$\gamma_{Fe}$
1	1190	-6.5	Magnetite	0.014	0.002	0.0004	0.658	0.029
2	1190	-6.75	Magnetite	0.017	0.001	0.0006	0.658	0.035
3	1190	-8.85	Magnetite	0.099	0.003	0.015	0.657	0.151
4	1190	-9.75	Wüstite	0.178	0.002	0.049	0.660	0.273
5	1190	-10.5	Wüstite	0.244	0.002	0.129	0.667	0.531
6	1190	-5	Magnetite	0.0021	0.0006	0.00004	0.663	0.020
7	1190	-11	Wüstite	0.300	0.003	0.245	0.655	0.817
8	1190	-3.9	Magnetite	0.0003	0.0003	0.000008	0.653	0.029
8R	1190	-3.9	Magnetite	0.0004	0.0007	0.000008	0.659	0.021
9	1190	-7.5	Magnetite	0.039	0.001	0.0019	0.661	0.049
10	1125	-10.5	Magnetite	0.188	0.002	0.047	0.661	0.252
11	1240	-8.75	Wüstite	0.130	0.002	0.029	0.667	0.220
12	1240	-9.5	Wüstite	0.217	0.002	0.075	0.690	0.346
13	1125	-11.1	Wüstite	0.227	0.002	0.102	0.650	0.450
14	1190	-8.25	Magnetite	0.066	0.001	0.0060	0.651	0.091
15	1240	-7.5	Magnetite	0.063	0.002	0.0051	0.658	0.080
16	1125	-9	Magnetite	0.069	0.001	0.0047	0.656	0.069

Table 1: Experimental results. Fe Oxide phase is calculated based on established phase diagrams for Fe and confirmed via electron microprobe analysis.  $1\sigma$  errors are values taken from repeat electron microprobe analysis. Pd/Au ratio is mole fractions of Pd and Au from electron microprobe analysis, with standard deviations of similar magnitude to those seen for Fe. Only run 12 shows a Pd/Au ratio significantly different from other samples. Gamma term is activity coefficient based on calculated activities of Fe at that temperature and oxygen fugacity and measured Fe content in the alloy.

Table 2

Oxide	Wt %	Component	Mole fraction	$\Delta G^0$	Activity
SiO <sub>2</sub>	50.34	SiO <sub>2</sub>	0.427457	1040.63	0.461304
TiO <sub>2</sub>	2.78	TiO <sub>2</sub>	0.02933		
Al <sub>2</sub> O <sub>3</sub>	13.78	Al <sub>2</sub> O <sub>3</sub>	0.128616		
Fe <sub>2</sub> O <sub>3</sub>	1.01	Fe <sub>2</sub> O <sub>3</sub>	0.00628		
Cr <sub>2</sub> O <sub>3</sub>	0.1	MgCr <sub>2</sub> O <sub>4</sub>	0.000653		
FeO	10.08	Fe <sub>2</sub> SiO <sub>4</sub>	0.069658	1888.07	0.094583
MnO	0.17	MnSi <sub>0.5</sub> O <sub>2</sub>	0.00238		
MgO	7.08	Mg <sub>2</sub> SiO <sub>4</sub>	0.086889		
NiO	0	NiSi <sub>0.5</sub> O <sub>2</sub>	0.00004		
CaO	11.5	CaSiO <sub>3</sub>	0.197753		
Na <sub>2</sub> O	2.36	Na <sub>2</sub> SiO <sub>3</sub>	0.037811		
K <sub>2</sub> O	0.53	KAlSiO <sub>4</sub>	0.011173		
P <sub>2</sub> O <sub>5</sub>	0.28	Ca <sub>3</sub> (PO <sub>4</sub> ) <sub>2</sub>	0.001959		

Table 2: Composition of Kilauea 1919 basalt (Garcia et al., 2003) used here and values produced by calculation using the MELTS algorithm. Normative components are calculated by MELTS at 1190°C and QFM-1.6. Values for  $\Delta G^0$  (in kJ/mol) are apparent values relative to the standard state at 298.15K and 1 bar, and must be corrected to the appropriate temperature for use in equation 6 using the data of Robie et al (1978). After this correction, using these values for the activity allowed for calculation of  $a_{Fe}$  via equation 6 and conversion into  $X_{Fe}$  using equations 4 and 5.

**FIGURE CAPTIONS**

Figure 1. Mole fractions of Fe measured in Au-Pd alloys after each experiment. Lines represent approximate boundary between wüstite (low  $f_{O_2}$ ) and magnetite at each temperature. Errors here are expected to be smaller than the size of the symbol (maximum  $2\sigma$  values  $\sim 0.2$  in  $f_{O_2}$  and  $\sim 0.01$  in Fe content).

Figure 2. Plot of activity-composition relationship based on calculated activities of Fe in wüstite or magnetite and measured alloy compositions.

Figure 3. Backscattered electron images of Samples 4 and 8R. Sample 4 (a) is a typical sample; lines are polishing features and black spots are dust or specks accumulated on surface. Sample 8R (b) shows the presence of an additional phase. The large dark spots are iron oxide crystals that formed during the reversal experiment. Electron probe measurements establish the phase to be magnetite.

Figure 4. Calculated  $RT \ln \gamma_{Fe}$  versus measured Fe content. Blue curve is the fit to the regular solution model presented in the text. All samples in this range show negative deviations from ideal solution, such that the value of  $\ln \gamma_{Fe}$  is negative. The solution model, however, predicts that at higher values of  $X_{Fe}$ , beyond those examined in this study, the value of  $\ln \gamma_{Fe}$  will become positive.

Figure 5(a). Composition of AuPd alloy calculated in equilibrium with Kilauea 1919 basalt at various values of oxygen fugacity. Data point is measured value of alloy

composition equilibrated with Kilauea 1919 basalt at QFM-1.6 (measured  $X_{\text{Fe}} = .114$ ).

5(b). Buffering capacity of a capsule in equilibrium with Kilauea 1919 basalt. Buffering capacity is defined here as the change in the mole fraction of Fe in the capsule per log unit change in oxygen fugacity. Under all but the most oxidizing conditions, a variation of a full log unit in oxygen fugacity should produce measurable changes in both alloy composition and measurable Fe loss or gain in the experiment itself.

## FIGURES

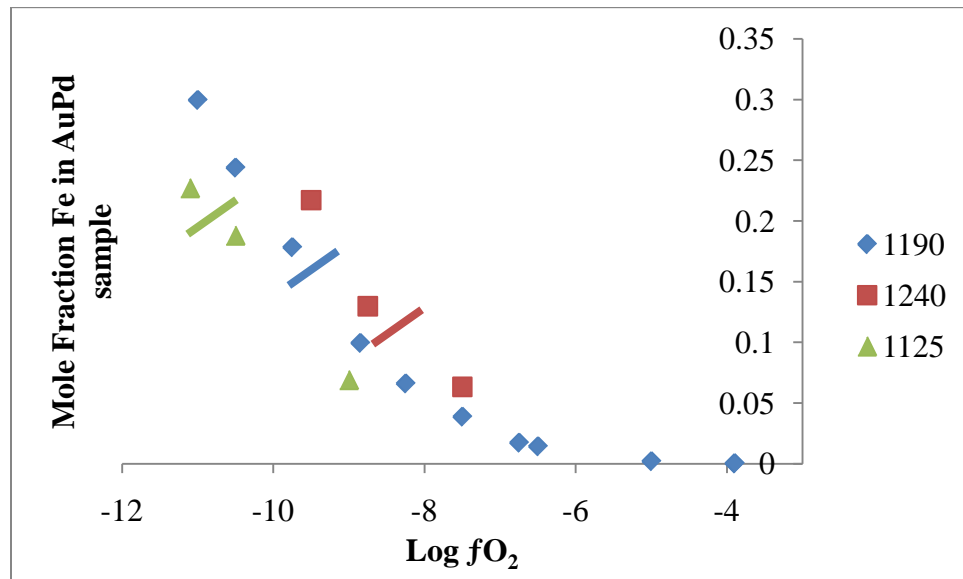


Figure 1

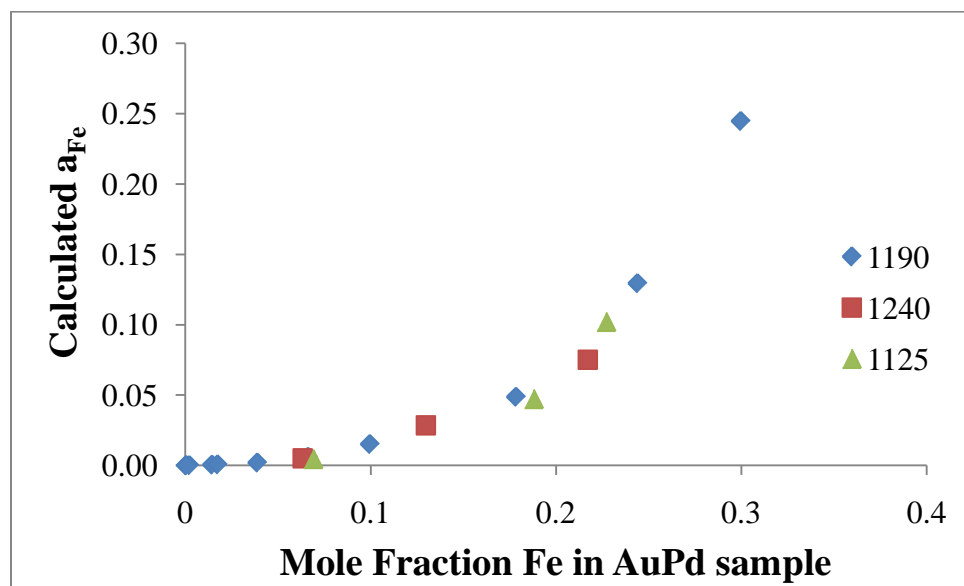


Figure 2

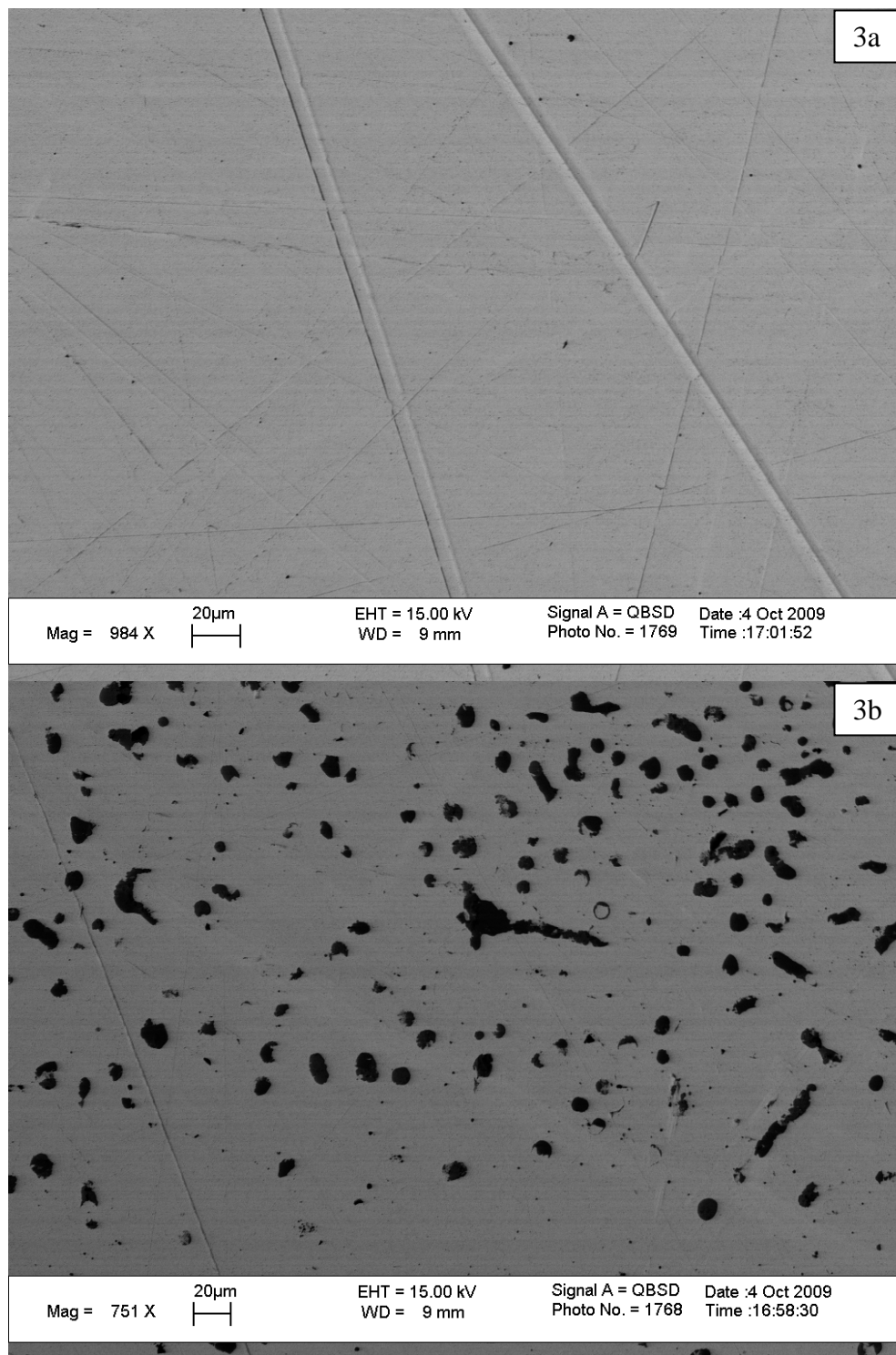


Figure 3

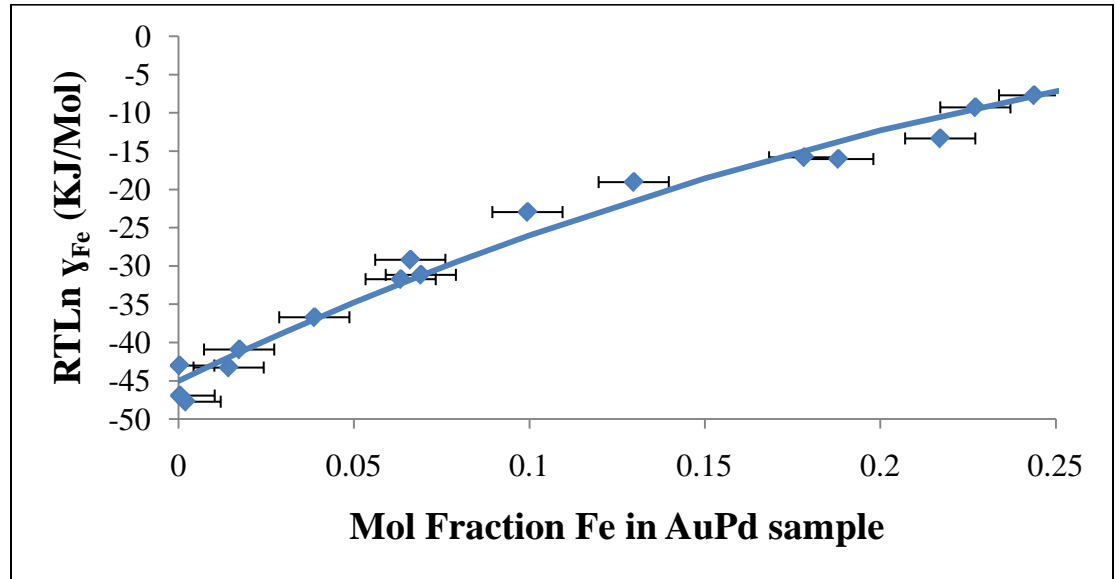


Figure 4

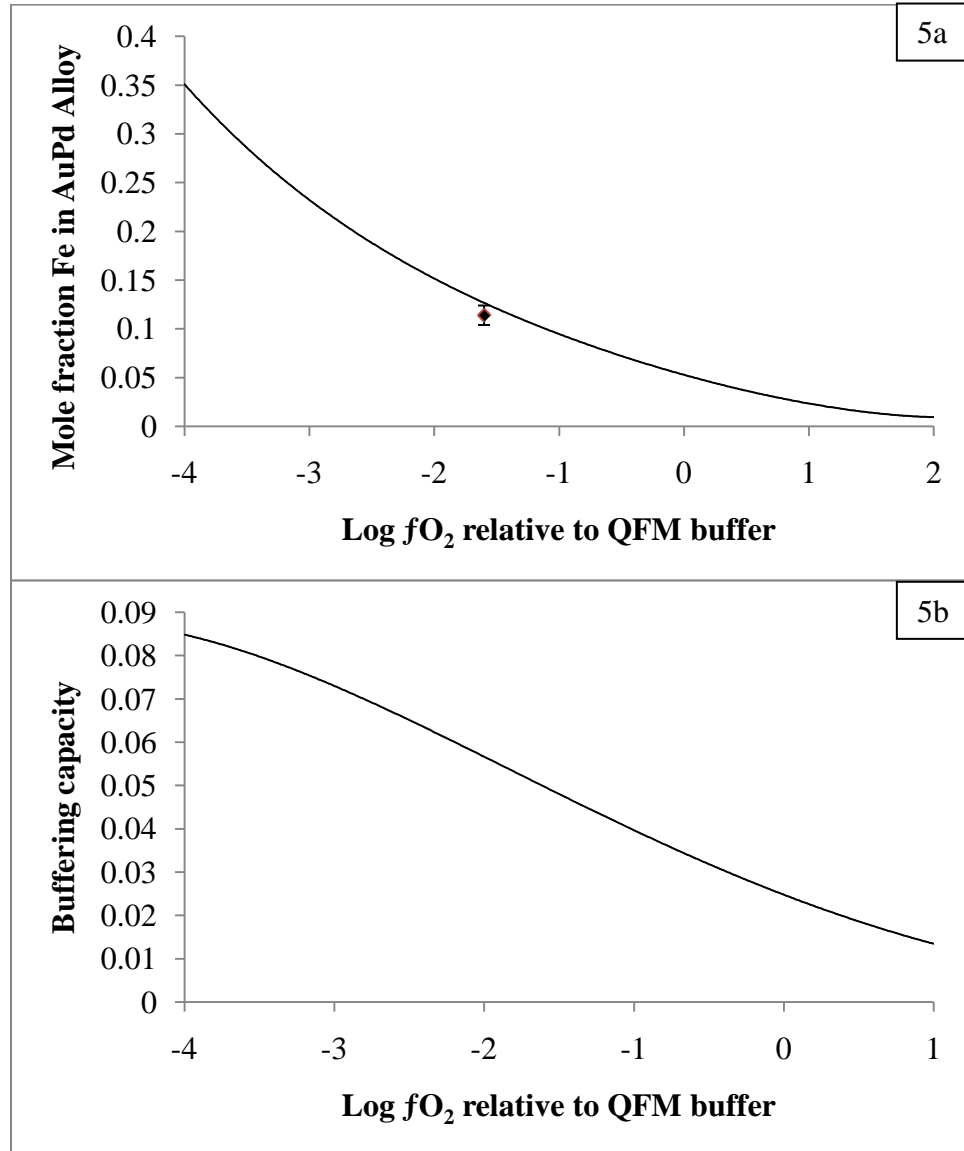


Figure 5.